Journal of Pharmaceutical and Biomedical Analysis 248 (2024) 116295

Contents lists available at ScienceDirect

Journal of Pharmaceutical and Biomedical Analysis

journal homepage: www.journals.elsevier.com/journal-of-pharmaceutical-and-biomedical-analysis

# Analytical quality by design-based development of a capillary electrophoresis method for Omeprazole impurity profiling

Adriana Modroiu [a,b], Luca Marzullo [b], Serena Orlandini [b,*], Roberto Gotti [c], Gabriel Hancu [a], Sandra Furlanetto [b]

[a] Department of Pharmaceutical and Therapeutic Chemistry, Faculty of Pharmacy, "George Emil Palade" University of Medicine, Pharmacy, Science and Technology of Târgu Mureş, Gh. Marinescu 38, Târgu Mureş 540142, Romania
[b] Department of Chemistry "U. Schiff", University of Florence, Via U. Schiff 6, Sesto Fiorentino, Florence 50019, Italy
[c] Department of Pharmacy and Biotechnology, University of Bologna, Via Belmeloro 6, Bologna 40126, Italy

ARTICLE INFO

*Keywords:*
Analytical quality by design
Capillary electrophoresis
Experimental design
Impurity profiling
Method operable design region
Omeprazole

ABSTRACT

Omeprazole (OME) is a proton pump inhibitor used to treat gastroesophageal reflux disease associated conditions. The current study presents an Analytical Quality by Design-based approach for the development of a CE method for OME impurity profiling. The scouting experiments suggested the selection of solvent modified Micellar ElectroKinetic Chromatography operative mode using a pseudostationary phase composed of sodium dodecyl sulfate (SDS) micelles and *n*-butanol as organic modifier in borate buffer. A symmetric three-level screening matrix $3^7//16$ was used to evaluate the effect of Critical Method Parameters, including Background Electrolyte composition and instrumental settings, on Critical Method Attributes (critical resolution values, OME peak width and analysis time). The analytical procedure was optimized using Response Surface Methodology through a Central Composite Orthogonal Design. Risk of failure maps made it possible to define the Method Operable Design Region, within which the following optimized conditions were selected: 72 mM borate buffer pH 10.0, 96 mM SDS, 1.45 %v/v *n*-butanol, capillary temperature 21 °C, applied voltage 25 kV. The method was validated according to ICH guidelines and robustness was evaluated using a Plackett-Burman design. The developed procedure enables the simultaneous determination of OME and seven related impurities, and has been successfully applied to the analysis of pharmaceutical formulations.

## 1. Introduction

Omeprazole (OME) belongs to the class of Proton-Pump Inhibitors (PPIs) used to reduce the production of stomach acid, being commonly prescribed to treat conditions such as gastroesophageal reflux disease, peptic ulcers and Zollinger-Ellison syndrome. As the pioneering compound in its class, it paved the way for the development of numerous other PPIs (lansoprazole, pantoprazole, rabeprazole) after its approval. OME is a benzimidazole derivative with a substituted pyridine ring; its chemical structure consists of a bicyclic structure with a chiral sulphur atom in the centre (Fig. 1) [1].

In the pharmaceutical industry, impurity profiling represents a pivotal aspect of Quality Control (QC) to ensure drug safety and efficacy. Impurity profiling encompasses both the detection and quantitation of various impurities, originating either from synthesis or degradation, which may be present in the drug substance or in the final drug product (DP) alongside the Active Pharmaceutical Ingredient (API) and excipients [2]. In the European Pharmacopoeia (Ph. Eur.), nine impurities for OME are listed from Impurity A to Impurity I (ImpA-ImpI) [3]. Ph. Eur. describes a RP-LC method for testing five OME impurities (ImpA-ImpE), based on C8 as stationary phase and a mobile phase composed of acetonitrile/phosphate buffer in a ratio of 27:73 v/v, with the last peak (ImpC) coming out over 30 min mark. ImpF and ImpG are not included among the compounds analysed by RP-LC and a separate UV-Vis spectroscopy method is described for their determination, as a sum of total absorbance. Several separation methods have been published in the literature for the quantification of OME and various sets of impurities. Their characteristics are summarized in Supplementary Table S1, encompassing considered analytes, type of technique, analysis time, presence of validation and type of sample. Most of these methods involve LC with UV detection [4–13] or MS detection [14], while only one CE method [15] and one high performance thin layer

* Corresponding author.
*E-mail address:* serena.orlandini@unifi.it (S. Orlandini).

https://doi.org/10.1016/j.jpba.2024.116295
Received 3 May 2024; Received in revised form 5 June 2024; Accepted 6 June 2024
Available online 7 June 2024

chromatography (HPTLC) method [16] have been reported.

While the most commonly employed technique for impurity profiling is LC, CE is gaining momentum in the field, owing to its high separation efficiency, many available operative modes, and high flexibility of its separation media, which include several pseudostationary phases as micelles, mixed micelles, microemulsions and cyclodextrins (CyDs). The Background Electrolyte (BGE) can be easily modified to accommodate for diverse pH values, by choosing different buffer types and concentrations and several additives. Other prominent strong points for CE are the microvolume of sample required, minimal reagents expenditure and the minute amounts of organic solvents employed, which alongside the strong preference for aqueous separation buffers and very low volume consumption (mL), translate into a greener and cheaper alternative to chromatography [2]. Different operative modes have recursively demonstrated their ability to be successfully applied to impurity profiling of pharmaceuticals, from Capillary Zone Electrophoresis (CZE) to Micellar ElectroKinetic Chromatography (MEKC), to MicroEmulsion ElectroKinetic Chromatography (MEEKC) and Non-Aqueous Capillary Electrophoresis (NACE) [2,17,18].

The aim of this research was the development of a CE method for accurately determining OME and its impurities ImpA-ImpE and ImpH-ImpI (Fig. 1), with the intention of using it in the routine QC of the DP. Following the approach used in Ph. Eur., ImpF and ImpG were not included among the considered compounds due to their extremely low solubility in common organic solvents and thus to the difficulty in achieving useful concentration values in the test sample. For these two compounds, Ph. Eur. provides a separate UV-Vis spectroscopy method. To our knowledge, the only CE method for the analysis of OME and its impurities involve the simultaneous determination of OME, ImpA, ImpC and 3 non pharmacopoeial related substances in bulk drug and was not fully validated [15]. In this study, to ensure a dependable method development, an advanced approach based on Analytical Quality by Design (AQbD) principles was adopted. This comprehensive and rational strategy incorporated both Design of Experiments (DoE) and Risk Assessment tools to enhance the reliability and robustness of the method.

The Quality by Design (QbD) paradigm, introduced in the 2000s, aimed to ensure the quality of pharmaceutical products and processes, with guidelines provided by the U.S. FDA and the International Council for Harmonisation (ICH) [19]. Subsequently, the principles of QbD were adapted to Analytical Procedures (APs) responsible for monitoring the quality of DPs, giving rise to AQbD. Over time, the interest in this area has steadily grown, with early papers pioneering the concept [20], followed by reviews, trends [21–25], and numerous applications in pharmaceutical analysis. A significant milestone occurred in 2023 when the ICH released Analytical Procedure Development Q14 [26] and Validation of Analytical Procedures Q2(R2) [27] guidelines, with the aim of specifying the development and validation activities necessary for the lifespan of an AP used to assess the quality of medicinal products. With the release of these documents, AQbD officially received recognition from regulatory bodies.

AQbD has found applications in pharmaceutical QC [23] and impurity profiling [28], with literature references highlighting its usage in CE for API related substances quantitation [29,30]. The CE optimization process involves a significant number of Critical Method Parameters (CMPs), hence AQbD is particularly advantageous in this field [25,31],

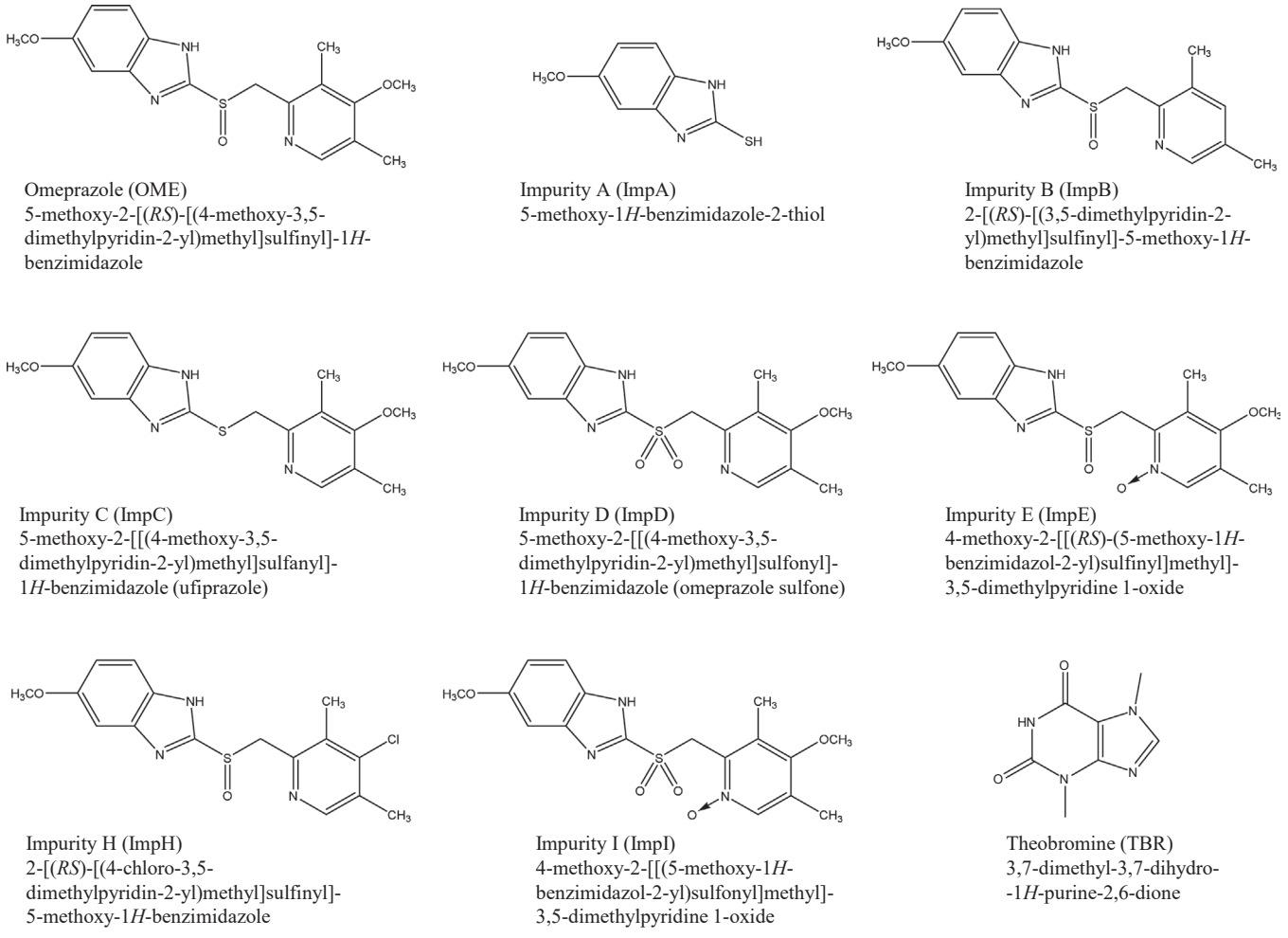


**Fig. 1.** Chemical structures of OME, considered OME impurities and internal standard theobromine.

since it enables a comprehensive examination of how CMPs influence Critical Method Attributes (CMAs), ultimately leading to the establishment of the Method Operable Design Region (MODR). This multivariate zone ensures that the CMAs meet specific requirements with a selected probability of failure. In this study, the development of the CE method was executed adhering to the new ICH guidelines, following all the steps outlined in the AQbD framework [21,25].

## 2. Materials and methods

### 2.1. Chemicals and reagents

OME was acquired from Alfa Aesar (Karlsruhe, Germany), while impurities ImpA, ImpB, ImpC, ImpD, ImpE, ImpF, ImpG, ImpH and ImpI were acquired from Aozeal (Alameda, CA, USA). Theobromine (TBR, Fig. 1), used as internal standard (IS), was purchased from Merck KGaA (Darmstadt, Germany).

The following CyDs were acquired from Sigma Aldrich (St. Louis, MO, USA): methyl-β-cyclodextrin (M-β-CyD, degree of substitution (DS) ~1.5–2.1), heptakis(2,3,6-tri-*O*-methyl)-β-cyclodextrin, (2-hydroxypropyl)-α-cyclodextrin (DS 0.6), (2-hydroxypropyl)-γ-cyclodextrin (DS 0.6), (2-hydroxyethyl)-β-cyclodextrin (HE-β-CyD, DS 0.7), 2-carboxymethyl-β-cyclodextrin sodium salt, 2-carboxyethyl-β-cyclodextrin sodium salt, sulphated-β-cyclodextrin sodium salt (S-β-CyD, DS ~7–11), γ-cyclodextrin. Heptakis(2,6-di-*O*-methyl)-β-cyclodextrin (DM-β-CyD) was from TCI (Tokyo, Japan); (2-hydroxypropyl)-β-cyclodextrin (HP-β-CyD, DS 0.6) was from Fluka (Buchs, Switzerland); sulfobutyl-β-cyclodextrin sodium salt (DS ~6.6) was from CyDex Pharmaceuticals (San Diego, CA, USA). All the other reagents, including boric acid, sodium tetraborate decahydrate (borax), sodium dodecyl sulphate (SDS), methanol (MeOH), *n*-butanol (nBuOH), phosphoric acid, acetic acid, 1 M NaOH were obtained from Sigma-Aldrich. Water was purified using a Millipore Simplicity 185 and Elix system (Billerica, MA, USA).

Omez® (Dr. Reddy's Laboratories, Bucharest, Romania) gastro-resistant capsules containing 20 mg OME were purchased from a local pharmacy.

### 2.2. Solutions and sample preparation

Standard stock solutions of OME (20 mg/mL) and of the related impurities ImpA, ImpB, ImpC, ImpD, ImpE, ImpH and ImpI (1 mg/mL) were prepared in MeOH and the IS TBR (0.5 mg/mL) was prepared in water. Stock solutions were stored at −20 °C in a freezer. Working standards were prepared immediately before use by dilution of the stock solutions with water.

The buffer solutions were prepared by mixing an appropriate volume of the specified 0.5 M acid or mixture of acids, adjusting the pH with 1 M NaOH and then filling up to the desired volume with water. The micellar phases were prepared by weighing the proper amount of SDS, adding it to the buffer and sonicating the mixtures for 5 min. CyDs and organic modifiers were subsequently added to the mixtures to obtain the desired BGE and were sonicated for other 5 min.

For the preparation of the OME capsules sample, the content of twenty capsules, labelled to contain 20 mg OME each, was mixed. The equivalent of 100 mg OME was accurately weighed and transferred in a beaker. 10 mL MeOH were added, obtaining a suspension which was stirred for 5 min. A 1 mL aliquot of the suspension was centrifuged and 100 μL of the supernatant were put in a 500 μL vial together with 40 μL of 0.5 mg/mL TBR and 360 μL water. OME test concentration was 2 mg/mL and TBR concentration was 0.04 mg/mL.

### 2.3. Instrumentation and CE analysis

Agilent 7100 CE System (Agilent Technologies, Waldbronn, Germany) with a UV-Vis DAD was used to carry out the experiments. The pH of the BGEs was measured using 713 pH Meter (Metrohm, Herisau, Switzerland). 50 μm i.d. fused-silica capillaries of 48.5 cm total length (40.0 cm effective length) purchased from CM Scientific Ryefield (Dublin, Ireland) were used. The new capillaries were rinsed with 1 M NaOH, 0.1 M NaOH, and water for 10 min each. Between the runs, the capillary was flushed with 1 M NaOH for 1 min, followed by 0.1 M NaOH for 1 min, water for 1 min, and BGE for 3 min. Hydrodynamic sample injection was performed at a pressure of 50 mbar for 4 s, followed by a BGE plug at 50 mbar for 4 s. UV detection was carried out at 200 nm. The temperature was set to 21 °C.

The CE working point, with the MODR interval in brackets, was the following: voltage, 25 kV (23–25 kV); BGE: 72 mM (65–80 mM) borate pH 10.00 (9.80–10.20), 96 mM (90–110 mM) SDS, 1.45 %v/v (1.04–1.75 %v/v) nBuOH.

### 2.4. Data analysis and software

OpenLab CDS ChemStation Edition (Agilent Technologies) software was used for instrument control, data acquisition and data evaluation. NemrodW software (NemrodW, LPRAI sarl, Marseille, France) was used for the DoE and the statistical analysis in the screening phase and in the robustness study, while MODDE Pro Version 13.0.2 (Sartorius Data Analytics, Göttingen, Germany) was used in the optimization phase and for the identification of MODR. The statistical analysis of the validation data was performed using Microsoft Excel (Microsoft Office 365, Redmond, CA, USA).

The DoE experimental runs were performed in a randomized order, analysing a test solution containing 2 mg/mL OME and 0.0200 mg/mL OME impurities (corresponding to 1 % OME). For building probability maps, the target for risk of error was set to ≤10 %, corresponding to a defect per million opportunities (DPMO) equal to 100,000 [32].

## 3. Results and discussion

### 3.1. Analytical target profile

The Analytical Target Profile (ATP) defines the specific objectives for the AP to be developed [26]. For this study, the ATP was set with the goal of concurrently measuring OME and its impurities for the QC of gastro-resistant capsules DP. Reasonable analysis time, namely suitable for the routine use of the AP in QC laboratory, and complete separation of the compounds were required. The predetermined acceptable thresholds for Validation Performance Criteria were established as follows.

For Selectivity, it was essential to achieve full separation of the analyte peaks and to ensure no overlapping or interference with the excipients present in the capsules. Quantitation Limit (QL) for the impurities was required ≤0.1 % w/w with respect to the API. The required Working Range for impurities was set from the QL up to 1 % relative to the API test concentration, while for the API the range was established between 80 % and 120 % of the specified test concentration. Concerning Accuracy, the expected recovery values were set between 98 % and 102 % for the API, and between 95 % and 105 % for the impurities. Regarding Precision, assessed as Repeatability, the API should present RSD values not exceeding 2 % and impurities should stay within 5 % RSD. At the QL, a higher RSD value of up to 15 % was deemed acceptable.

### 3.2. Knowledge management

OME is an amphoteric compound with $pK_a$ values of 14.7 (dissociation of the hydrogen from the 1 position of the benzimidazole ring) and of 7.1 (dissociation from the protonated pyrimidine nitrogen) [33]. Knowledge Management [26] involved the execution of scouting experiments to identify the suitable CE operative mode, including choice of buffer, surfactant and other additives, in order to approach the ATP.

Considering the low stability of PPIs in acidic conditions, the

scouting experiments started with a MEKC system composed of 20 mM borax buffer containing 80 mM SDS. In these preliminary runs the sample solution contained 0.1 mg/mL OME and 0.02 mg/mL impurities; OME concentration was kept low in order to obtain a clear indication of the electrophoretic behaviour of the analytes by reducing the risk of overlap due to the overwhelming area of OME with respect to impurities when applying the final test concentration (2 mg/mL). The main challenging analytical points were identified in the following issues:

i) narrow migration window, where the majority of the peaks could be only distinguished but not separated, with the higher critical issue observed for the separation between OME and ImpB, compounds which only differ in a methoxy group;
ii) low efficiency of the peaks, especially OME peak.

Hence, several modifications were made to the initial MEKC system. Sodium cholate was also evaluated as surfactant replacing SDS, but the obtained results were not satisfactory. Buffer pH was tested at three levels (8.20, 9.20 and 10.20) using a 30 mM borate buffer with 75 mM SDS, the best separation being observed at pH 9.20 (Supplementary Fig. S1a). At this pH value, several types of buffers were also tried: 30 mM borate, borate/phosphate, and Britton Robinson (acetate/borate/phosphate) with the addition of 80 mM SDS; however, none of them yielded better results. The addition of nBuOH at three levels of concentration (0.5, 1.0 and 2.0 %v/v) to 20 mM borax buffer containing 80 mM SDS was also investigated. In this case, a positive and significant effect on the peak shapes and on the separation was observed, especially between ImpB and OME. Percentages of nBuOH higher than 2.0 %v/v resulted in longer migration times, without further relevant improvements in the electropherogram. Furthermore, a variety of CyDs, as listed in Section 2.1, was evaluated at two concentration levels (10–25 mM), but only a few of them yielded some improvement of the separation of the analytes, specifically: M-β-CyD, DM-β-CyD, HE-β-CyD, HP-β-CyD and S-β-CyD. Replicate injections were performed for assessing the stability of the separation with CyD-modified BGE, yielding only DM-β-CyD as a solid candidate for further development.

Other operative modes were also evaluated: CZE at different pH values (50 mM phosphate at pH 2.5, 50 mM acetate at pH 4.0, 50 mM phosphate at pH 7.0); MEEKC, with a standard microemulsion composed of 90.96 % 80 mM borate pH 9.20, 1.00 % *n*-heptane, 5.38 % *n*-butanol and 2.66 % SDS (Supplementary Fig. S1b). The possibility of operating in reverse polarity by MEKC (Supplementary Fig. S1c) and MEEKC was also considered, focusing on acidic pH by using 100 mM phosphate buffer at pH 2.5. Nevertheless, none of these systems provided better separations than nBuOH-modified MEKC.

Therefore, a nBuOH-modified MEKC system using normal polarity was selected and DM-β-CyD was chosen as additive to be further evaluated due to the better OME peak shape and faster migration time. *n*-butanol has been demonstrated to play a pivotal role in tuning the separation in solvent-modified MEKC, as previously reported [34]. The different effects can be summarized not only in the modulation of the dielectric constant and the viscosity of the BGE, but also in the modification of the affinity of the analytes for the micellar pseudostationary phase by forming mixed SDS/nBuOH micelles, and in the change of the affinity of the analytes for the aqueous phase.

### 3.3. Risk Assessment and critical method parameters

Risk Assessment was performed by means of an Ishikawa diagram (not shown), which was drawn to be superimposable with the one reported in Ref. [29] for evaluating the main possible sources of variation in an AP consisting of MEKC with the addition of an organic modifier and a CyD. The parameters involved in separation and detection, capillary, injection phase and BGE composition were investigated to identify the CMPs to be further studied by DoE. From the preliminary scouting experiments, it was possible to fix the hydrodynamic injection (50 mbar for 4 s), capillary type and length (50 μm i.d., bare-fused silica, 48.5 cm total length, 40.0 cm effective length) and detection wavelength (200 nm). Type of buffer (borate), type of surfactant (SDS), type of CyD (DM-β-CyD) and type of organic modifier (nBuOH) to be employed were also chosen. Seven CMPs, for which a more detailed study by DoE was needed, were selected as follows: concentration of borate buffer (*Buffer conc*), buffer pH (*pH*), SDS concentration (*SDS conc*), organic modifier concentration (*BuOH conc*), DM-β-CyD concentration (*CyD conc*), voltage (*V*) and temperature (*T*).

### 3.4. Screening phase

The screening phase involved the study of the effects of the seven CMPs shown in Supplementary Table S2. The experimental domain of each CMP was carefully selected based on the preliminary experiments to achieve reasonable analysis time and a suitable separation current value, while keeping Knowledge Space as wide as possible. As for *CyD conc* levels, to gain a better understanding of the CyD effects on the separation, a zero (absence) value was included among the studied levels (0–10–20 mM) to postpone the choice of whether adding DM-β-CyD to the BGE after the screening phase results. In fact, before running the screening experiments it was not clear if the final optimized conditions would include or not DM-β-CyD in the BGE, because the presence of CyD decreased analysis time, but its actual capability of increasing resolution between ImpB/OME needed further scrutiny.

All the CMPs were investigated at three levels and the Free-Wilson model which was hypothesized for linking the CMPs to the CMAs is reported below:

$$y=A_0+A_1A+A_2A+B_1B+B_2B+C_1C+C_2C+D_1D+D_2D+E_1E+E_2E+F_1F+F_2F+G_1G+G_2G$$

where *y* is the response (each CMA), $A_0$ is the constant term, *A* is *pH*, *B* is *Buffer conc*, C is *SDS conc*, D is *BuOH conc*, E is *CyD conc*, F is *V* and G is *T*. For each CMP, coefficients in the model are present in number of two, value which corresponds to the number of investigated levels minus one. A $3^7//16$ symmetric screening matrix, presented in Table 1, was selected for evaluating the effects of the distinct levels of the CMPs on the CMAs.

Through observation of the screening results, some general considerations could be drawn, and particular issues were noticed as described below:

i) the values of measured current were satisfactory all throughout the screening design, as they ranged from 35 μA (exp. no. 10) to 119 μA (exp. no. 3);
ii) The addition of DM-β-CyD led in some cases to partial enantioseparation of the racemate impurities (ImpB, ImpE, ImpH), resulting in a confounded electrophoretic pattern and in the loss of certain information on the identity of the peaks, potentially exacerbated by possible inversion in the migration order of the compounds. Due to this effect, the assignment of identities to all the peaks was not performed in this phase and was postponed to subsequent Response Surface Methodology (RSM) studies. The partial splitting in two peaks would lead in turn to an increase in the Quantitation Limit and Detection Limit of the corresponding analyte, and thus to a decrease of method sensitivity. Moreover, in certain experiments (no. 2, 4, 8, 16) partial peak splitting of OME (beginning of enantioseparation) was observed, leading to a consequent peak asymmetry/broadening, which was detrimental for both efficiency and reliability of peak integration. Both of these DM-β-CyD effects were undesirable, as the first one could lead to a decrease of sensitivity in impurity detection/quantitation and the second one could result in a decrease of OME peak efficiency due to its deteriorated and widened peak shape;

**Table 1**
Screening phase: $3^7$//16 symmetric screening matrix.

| No. exp. | *pH* | *Buffer conc* (mM) | *SDS conc* (mM) | *BuOH conc* (%v/v) | *CyD conc* (mM) | *V* (kV) | *T* (°C) | $R_6$ | $W_{OME}$ (min) | *t* (min) |
|---|---|---|---|---|---|---|---|---|---|---|
| 1 | 8.20 | 75 | 90 | 1.50 | 10 | 27 | 24 | 1.04 | 0.19 | 8.55 |
| 2 | 10.20 | 50 | 90 | 1.00 | 20 | 24 | 24 | 0.00 | 0.24 | 7.01 |
| 3 | 10.20 | 100 | 70 | 1.00 | 10 | 27 | 21 | 0.00 | 0.16 | 8.14 |
| 4 | 9.20 | 100 | 110 | 0.50 | 10 | 24 | 24 | 0.00 | 0.54 | 10.33 |
| 5 | 10.20 | 75 | 110 | 1.50 | 0 | 24 | 21 | 3.68 | 0.13 | 16.39 |
| 6 | 9.20 | 100 | 90 | 1.50 | 20 | 21 | 21 | 1.59 | 0.19 | 11.28 |
| 7 | 9.20 | 75 | 110 | 1.00 | 20 | 27 | 18 | 0.74 | 0.23 | 8.30 |
| 8 | 9.20 | 75 | 90 | 1.00 | 10 | 24 | 21 | 0.00 | 0.33 | 9.37 |
| 9 | 10.20 | 75 | 90 | 0.50 | 10 | 21 | 18 | 1.32 | 0.32 | 14.02 |
| 10 | 8.20 | 100 | 90 | 1.00 | 0 | 24 | 18 | 0.00 | 0.31 | 12.65 |
| 11 | 8.20 | 50 | 110 | 1.00 | 10 | 21 | 21 | 0.89 | 0.28 | 14.53 |
| 12 | 9.20 | 50 | 70 | 1.50 | 10 | 24 | 18 | 0.72 | 0.20 | 8.37 |
| 13 | 8.20 | 75 | 70 | 0.50 | 20 | 24 | 21 | 1.00 | 0.17 | 8.50 |
| 14 | 9.20 | 50 | 90 | 0.50 | 0 | 27 | 21 | 0.00 | 0.22 | 7.75 |
| 15 | 9.20 | 75 | 70 | 1.00 | 0 | 21 | 24 | 0.00 | 0.32 | 11.39 |
| 16 | 9.20 | 75 | 90 | 1.00 | 10 | 24 | 21 | 0.00 | 0.44 | 9.39 |

$R_6$, resolution ImpB/OME; $W_{OME}$, OME 5σ peak width at 4.4 % peak height; *t*, analysis time, measured as the migration time of the last migrating impurity.

iii) The resolution between ImpB and OME was confirmed to be a critical response, as there was a complete overlap of ImpB and OME in half of the experiments.

Thus, the screening phase aimed to produce a clear electrophoretic profile where the separation of enantiomers for chiral compounds was prevented, to improve method sensitivity for the impurities and to obtain a sharper OME peak shape. The baseline resolution of all the compounds should be achieved, while keeping analysis time as low as possible. Therefore, the CMAs were chosen as critical resolution between ImpB and OME ($R_6$), OME 5σ width at 4.4 % peak weight ($W_{OME}$) and analysis time (*t*).

The models for each of the three CMAs were found significant by ANOVA and the obtained graphical analysis of effects is plotted in Fig. 2: $R_6$ in Fig. 2a,b, $W_{OME}$ in Fig. 2c,d and *t* in Fig. 2e,f. The plots on the left side (Fig. 2a,c,e) indicate whether the detected effect on the CMA is significant when stepping from one factor level to another. Pairs of factor levels were considered, so that for each CMA three bars are observed, referring to the differences of effects between levels 2 and 1 (b1/2–1), levels 3 and 1 (b1/3–1), levels 3 and 2 (b1/3–2). If the changes of levels cause a significant effect on the CMA, the bars are coloured in orange. The plots on the right side (Fig. 2b,d,f) show the effect of each level on the response, and for each CMA the three levels are shown with different colours: blue for the lowest level, green for the medium level and red for the highest level. The length of the bars is related to the magnitude of the effect, indicating that a longer bar represents a larger impact on the response variable.

As for $R_6$ plots (Fig. 2a,b), it was clear that the most influential factors were *SDS conc* and *BuOH conc*, meaning that the SDS micellar system, modified with nBuOH, was pivotal in obtaining the separation; for both of these CMPs the best results were obtained at high levels. An increase in resolution could be also achieved choosing a high level of *pH* and a medium level of *Buffer conc*. As expected, an increase of *V* led to a reduction of the resolution. Although the medium level of *T* had a lesser impact compared to other factors related to the BGE, it contributed to maximizing $R_6$.

Looking at $W_{OME}$ (Fig. 2c,d), the best results were achievable at high *pH* value as well, but on the other hand, low levels of *Buffer conc* and *SDS conc* were preferred. *BuOH conc* was very influential on this CMA, with a high level of this factor favouring a sharper peak. A high setting for *V* and a medium setting for *T* proved to be the most effective.

Finally, concerning *t* (Fig. 2e,f), each CMP was found to exert a significant effect. The levels that resulted in minimizing this response were a medium level for *pH* and a low level for *buffer conc*, *SDS conc* and *BuOH conc*. As expected, *V* and *T* had to be set at high levels to achieve minimal values of *t*.

A separate discussion should be made for *CyD conc* effect. In fact, its importance on $R_6$ was limited compared to other BGE factors such as *SDS conc* and *BuOH conc*. However, the addition of DM-β-CyD was undoubtedly effective in reducing *t*. Despite this, it was decided to discard its addition to the BGE mainly due to the drawbacks reported above (enantiomer separation with consequent loss of sensitivity, OME peak

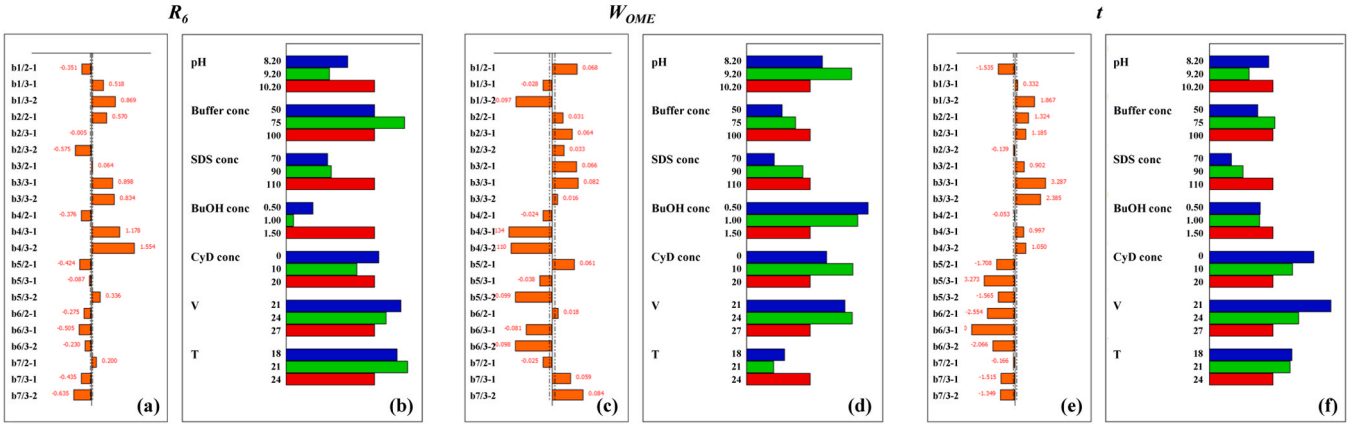


**Fig. 2.** Screening graphical analysis of effects for each studied CMA. $R_6$, resolution ImpB/OME; $W_{OME}$, OME 5σ peak width; *t*, analysis time, corresponding to the migration time of the last migrating peak.

broadening with consequent loss of efficiency, possible inversion of migration order of compounds). This also led to advantages in terms of simplicity of the BGE formulation and lower costs of analysis.The other fixed factor was *T*, whose chosen value was at the medium level (21 °C) for its beneficial effects on $R_6$ and $W_{OME}$. For *pH* and *Buffer conc* the RSM experimental domain was reduced to a narrower range inside the screening domain, aiming to find a compromise among the CMAs. However, for *SDS conc*, *BuOH conc* and *V*, the new RSM domain included values outside the original range, to further increase $R_6$.

### 3.5. Response surface methodology

The five CMPs for which further in-depth investigation by RSM was undertaken are summarized in Supplementary Table S2 together with the new corresponding experimental domain.

A quadratic polynomial model was hypothesized for describing the mathematical relationship between the CMPs ($x_i$) and the CMAs ($y$) according to the following equation:

$$y = \beta_0 + \beta_1 x_1 + \beta_2 x_2 + \beta_3 x_3 + \beta_4 x_4 + \beta_5 x_5 + \beta_{11} x_1^2 + \beta_{22} x_2^2 + \beta_{33} x_3^2 + \beta_{44} x_4^2 + \beta_{55} x_5^2 + \beta_{12} x_1 x_2 + \beta_{13} x_1 x_3 + \beta_{14} x_1 x_4 + \beta_{15} x_1 x_5 + \beta_{23} x_2 x_3 + \beta_{24} x_2 x_4 + \beta_{25} x_2 x_5 + \beta_{34} x_3 x_4 + \beta_{35} x_3 x_5 + \beta_{45} x_4 x_5 + \varepsilon$$

In this model the CMPs are indicated by $x_1$ (*Buffer conc*), $x_2$ (*pH*), $x_3$ (*SDS conc*), $x_4$ (*BuOH conc*) and $x_5$ (*V*). The model contains the intercept ($\beta_0$), the linear terms ($\beta_i$), the quadratic terms ($\beta_{ii}$) and the first-order interaction terms ($\beta_{ij}$), and $\varepsilon$ represents the experimental error.

The coefficients of the model were estimated by an Orthogonal Central Composite Design (OCCD), which requires the experimental domain of the factors to be fractionated at five levels (-α, −1, 0, +1, +α), with α=1.66. The OCCD experimental plan, along with the measured CMAs values, is reported in Table 2.

Some general remarks could be made on the OCCD results. First, a general increase of analysis time (from 11.14 to 22.69 min) compared to the screening runs (from 7.01 to 16.39 min) was observed. This was expected due to the absence of DM-β-CyD in the BGE, which contributed to speed up the analysis. On the other side, a remarkable increase in the separation between ImpB and OME peaks was obtained, since they were either partially or fully resolved in the majority of OCCD experiments, aside from only five runs (no. 1, 2, 5, 6, 19), which were all characterized by low values of pH. The migration order of the compounds remained the same in all the runs and no issues were found about interpreting the electrophoretic pattern in terms of peak identities. However, an unexpected issue arose for the separation between the last migrating peaks, ImpH and ImpC (resolution $R_8$). A high variability in the separation was noticed, as confirmed by the measured values, which ranged from 0 to 28.06. Hence, this response was selected as fourth CMA and was included in the RSM statistical evaluation.

The responses were statistically treated, without the need for mathematical transformation, and the models were refined by deletion of non-significant interaction and quadratic coefficients. All of them were found to be valid and significant by ANOVA and were characterized by good quality parameters (Supplementary Table S3) [32]. The coefficient of determination $R^2$ and of goodness of prediction $Q^2$ fell within the ranges 0.9368–0.9958 and 0.7645–0.9825, respectively.

Graphical analysis of effects was performed, and the related plots are shown in Supplementary Fig. S2a-d. The length of the bars is proportional to the weight of the coefficient, while the confidence interval for the coefficient is represented by the error bar. An overwhelmingly positive effect of pH was highlighted on both resolution $R_6$ (Supplementary Fig. S2a) and $R_8$ (Supplementary Fig. S2b), demonstrating that a correct setting of this factor at high values was very important to increase selectivity. Interestingly, *BuOH conc* had an important positive effect on both the CMAs, while the effect of *SDS conc* was not significant in the investigated domain. *Buffer conc* exerted a significant linear positive effect on $R_8$, even if to a much lesser extent than those of *pH* and *BuOH conc*. It is also worthwhile to note that a positive quadratic effect of pH was highlighted for both the resolutions. Some significant positive interactions were also found (for $R_6$, *Buffer conc*BuOH conc;* for $R_8$, *Buffer conc*pH* and *pH*BuOH conc*), even if they were of limited importance. As for $W_{OME}$ (Supplementary Fig. S2c), a high influence of *V* was observed together with a negative quadratic effect of *pH*, and some

**Table 2**
Response surface methodology: orthogonal central composite design.

| No. exp. | *Buffer conc* (mM) | *pH* | *SDS conc* (mM) | *BuOH conc* (%v/v) | *V* (kV) | $R_6$ | $R_8$ | $W_{OME}$ (min) | *t* (min) |
|---|---|---|---|---|---|---|---|---|---|
| 1 | 69 | 9.08 | 96 | 0.95 | 24 | 0.00 | 1.06 | 0.27 | 11.14 |
| 2 | 81 | 9.08 | 96 | 0.95 | 20 | 0.00 | 1.08 | 0.37 | 15.04 |
| 3 | 69 | 9.92 | 96 | 0.95 | 20 | 1.32 | 10.98 | 0.40 | 17.06 |
| 4 | 81 | 9.92 | 96 | 0.95 | 24 | 1.16 | 15.67 | 0.30 | 14.74 |
| 5 | 69 | 9.08 | 114 | 0.95 | 20 | 0.00 | 0.99 | 0.34 | 15.63 |
| 6 | 81 | 9.08 | 114 | 0.95 | 24 | 0.00 | 1.42 | 0.29 | 13.12 |
| 7 | 69 | 9.92 | 114 | 0.95 | 24 | 1.43 | 11.22 | 0.24 | 13.65 |
| 8 | 81 | 9.92 | 114 | 0.95 | 20 | 1.39 | 13.17 | 0.43 | 22.03 |
| 9 | 69 | 9.08 | 96 | 1.55 | 20 | 0.58 | 1.76 | 0.35 | 15.70 |
| 10 | 81 | 9.08 | 96 | 1.55 | 24 | 0.61 | 2.13 | 0.29 | 13.08 |
| 11 | 69 | 9.92 | 96 | 1.55 | 24 | 1.84 | 19.28 | 0.21 | 14.19 |
| 12 | 81 | 9.92 | 96 | 1.55 | 20 | 2.26 | 21.12 | 0.33 | 22.69 |
| 13 | 69 | 9.08 | 114 | 1.55 | 24 | 0.53 | 1.95 | 0.30 | 13.64 |
| 14 | 81 | 9.08 | 114 | 1.55 | 20 | 0.61 | 2.22 | 0.40 | 19.17 |
| 15 | 69 | 9.92 | 114 | 1.55 | 20 | 1.44 | 17.59 | 0.40 | 21.97 |
| 16 | 81 | 9.92 | 114 | 1.55 | 24 | 2.09 | 22.58 | 0.26 | 18.40 |
| 17 | 65 | 9.50 | 105 | 1.25 | 22 | 0.75 | 4.09 | 0.32 | 14.76 |
| 18 | 85 | 9.50 | 105 | 1.25 | 22 | 0.85 | 6.66 | 0.38 | 17.48 |
| 19 | 75 | 8.80 | 105 | 1.25 | 22 | 0.00 | 0.00 | 0.32 | 14.09 |
| 20 | 75 | 10.20 | 105 | 1.25 | 22 | 2.82 | 28.06 | 0.21 | 19.09 |
| 21 | 75 | 9.50 | 90 | 1.25 | 22 | 0.75 | 5.16 | 0.34 | 14.43 |
| 22 | 75 | 9.50 | 120 | 1.25 | 22 | 0.84 | 5.95 | 0.37 | 17.74 |
| 23 | 75 | 9.50 | 105 | 0.75 | 22 | 0.44 | 2.94 | 0.40 | 14.82 |
| 24 | 75 | 9.50 | 105 | 1.75 | 22 | 1.46 | 8.46 | 0.32 | 17.49 |
| 25 | 75 | 9.50 | 105 | 1.25 | 19 | 0.72 | 4.83 | 0.45 | 20.12 |
| 26 | 75 | 9.50 | 105 | 1.25 | 25 | 0.81 | 6.06 | 0.28 | 12.96 |
| 27 | 75 | 9.50 | 105 | 1.25 | 22 | 0.82 | 5.94 | 0.34 | 16.01 |
| 28 | 75 | 9.50 | 105 | 1.25 | 22 | 0.66 | 4.87 | 0.36 | 15.88 |
| 29 | 75 | 9.50 | 105 | 1.25 | 22 | 0.71 | 5.20 | 0.38 | 16.03 |

R6, resolution ImpB/OME; R8, resolution ImpH/ImpC; WOME, OME 5σ peak width at 4.4 % peak height; t, analysis time, measured as ImpC migration time.

interactions of lower extent were also recorded. Finally, all the linear terms of the CMPs were significant on *t* (Supplementary Fig. S2d), all exerting a positive effect apart from *V*, as expected. Several interactions coefficients were also found to be significant, but with much lower weight compared to linear terms.

The CMA models were graphically represented through the contour plots reported in Supplementary Figures S3-S6. The plots were drawn by reporting *BuOH conc vs. pH* at three *Buffer conc* levels (65, 75 and 85 mM) and three *V* levels (19, 22 and 25 kV), while keeping the value of *SDS conc* at the central point of its experimental domain (105 mM). The dotted highlighted lines corresponded to the target values, namely the CMA thresholds (minimum or maximum value accepted). The CMAs thresholds were set as follows: $R_6 \geq 1.3$, $R_8 \geq 2.0$, $W_{OME} \leq 0.34$ min and $t \leq 17$ min. The target of 1.3 for $R_6$ had been already selected in the screening phase based on the visual inspection of the electropherograms (as effectively bringing baseline separation of the involved compounds), while the target of 2.0 for $R_8$ corresponded to a baseline separation for peaks of similar characteristics of width and height (i.e., ImpH and ImpC). As for the other CMAs, the selection of the target was made based on the statistics, choosing a value just above the median of the RSM measured values, which was considered acceptable for the analysis.

Comparing the graphs for $R_6$ (Supplementary Fig. S3) and $R_8$ (Supplementary Fig. S4), it can be pointed out that the trend of these responses is quite similar, with higher values of resolution located at high levels of *pH*, *BuOH conc* and *Buffer conc*. Nevertheless, the zone with predicted values inside the thresholds is much wider in the case of $R_8$.

As for $W_{OME}$ contour plots (Supplementary Fig. S5), a strong curvature could be noticed, due to the prominent quadratic effect of pH. Additionally, using a high voltage setting (25 kV), the area on the plot corresponding to accepted values spanned the entire experimental range. Anyway, when the voltage was lowered to 22 kV, this area shrank considerably, and at 19 kV it was confined only to the edges of the experimental domain for *pH* and *BuOH conc*.

Finally, concerning the contour plots drawn for *t* (Supplementary Fig. S6), the best results were located at low *pH*, low *BuOH conc*, low *Buffer conc* and high *V*. As it was observed for $W_{OME}$, the area of the acceptable zone was strongly shrunk stepping from 25 kV to 19 kV.

The contour plots of the four CMAs were merged by overlapping to obtain the sweet spot plot that is shown in Fig. 3. This plot makes it possible to identify at a first glance the zone (the "sweet spot") where all the CMAs' requirements were met based on their average predicted values. In particular, the colour scale is used to identify the zones where none of the CMAs (white), one CMA (orange), two (yellow), three (light green) or four CMAs (brilliant green) are inside the thresholds. No brilliant green zones could be found at low voltage value (19 kV); on the other hand, they covered a notable area of the experimental space at high (25 kV) and medium (22 kV) voltage values, provided that a low *Buffer conc* value was set.

### 3.6. Method operable design region

The MODR was identified by means of the calculated models and by Monte-Carlo simulations [35], which account for model error. A robust set-point was sought to establish a multivariate space hypervolume, within which all the CMAs specifications were fulfilled according to an acceptance limit of 10 % (DPMO 100,000), meaning that 90 % of the samples are within limits. The robust set-point corresponded to the following analytical conditions: *Buffer conc*, 72 mM; *pH*, 10.01; *SDS conc*, 96 mM; *BuOH conc*, 1.48 %v/v; *V*, 24 kV. The probability maps are shown in Fig. 4, where the MODR is highlighted in green and is included in the 10 % isoresponse lines.

As expected from the previous observation of the sweet spot plot (Fig. 3), the optimum working conditions should necessarily include high values of *V*, since the maps reported in the second row (22 kV) and in the third row (19 kV) showed limited or no brilliant green area. The final optimized conditions were very similar to the robust set-point, which was slightly modified to prepare the BGE in a more practical way; the only significant difference from the robust conditions was the increase of *V* from 24 kV to 25 kV, to obtain a lower analysis time. Therefore, the chosen working point with the related MODR was the following: *Buffer conc*, 72 mM (65–80 mM); *pH*, 10.00 (9.80–10.20); *SDS conc*, 96 mM (90–110 mM); *BuOH conc*, 1.45 %v/v (1.04–1.75 %v/v); *V*, 25 kV (23–25 kV) (Supplementary Table S2). The typical electropherogram under the working point conditions was characterized by a current of 73 μA and analysis time lower than 14 min (Fig. 5).

### 3.7. Robustness and method control

The robustness of the AP was assessed before its validation, following recommendations outlined in ICH guideline Q14 [26]. The guideline emphasizes the significance of evaluating this parameter during development phase, since it is of paramount importance for the AP lifecycle, representing a measure of the AP's capacity to meet the expected performance requirements during normal use. Hence, small yet deliberate

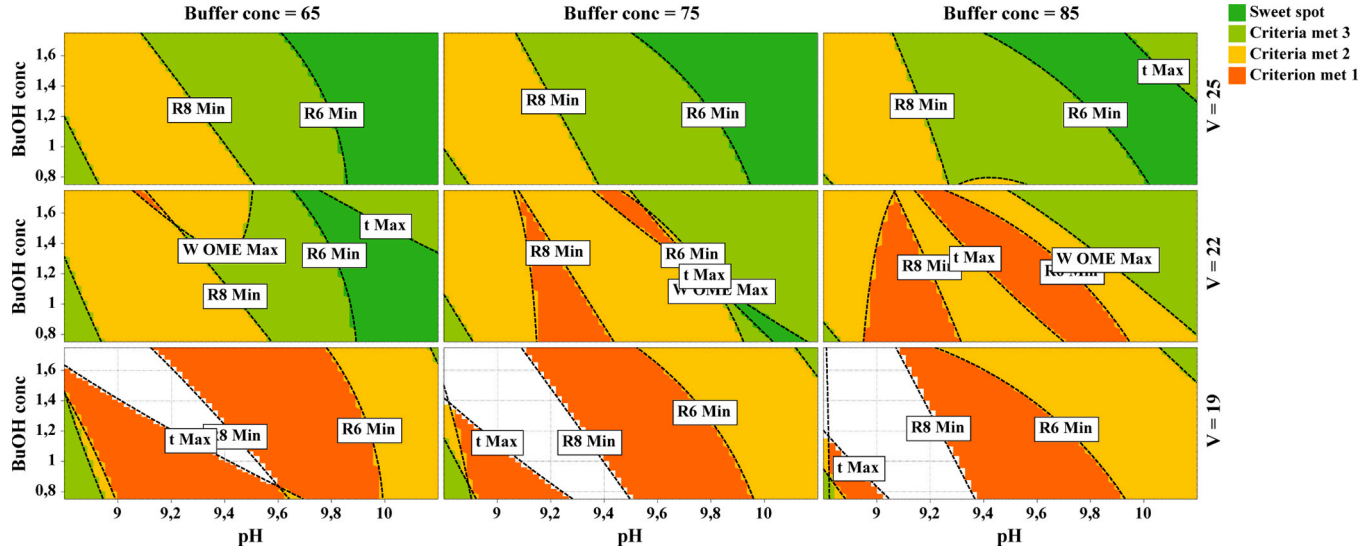


**Fig. 3.** Sweet spot plot, plotting *BuOH conc vs. pH* at three different levels of *Buffer conc* and *V*, with *SDS conc* fixed at 105 mM. Targets: $R_6 \geq 1.3$, $R_8 \geq 2.0$, $W_{OME} \leq 0.34$ min and $t \leq 17$ min.

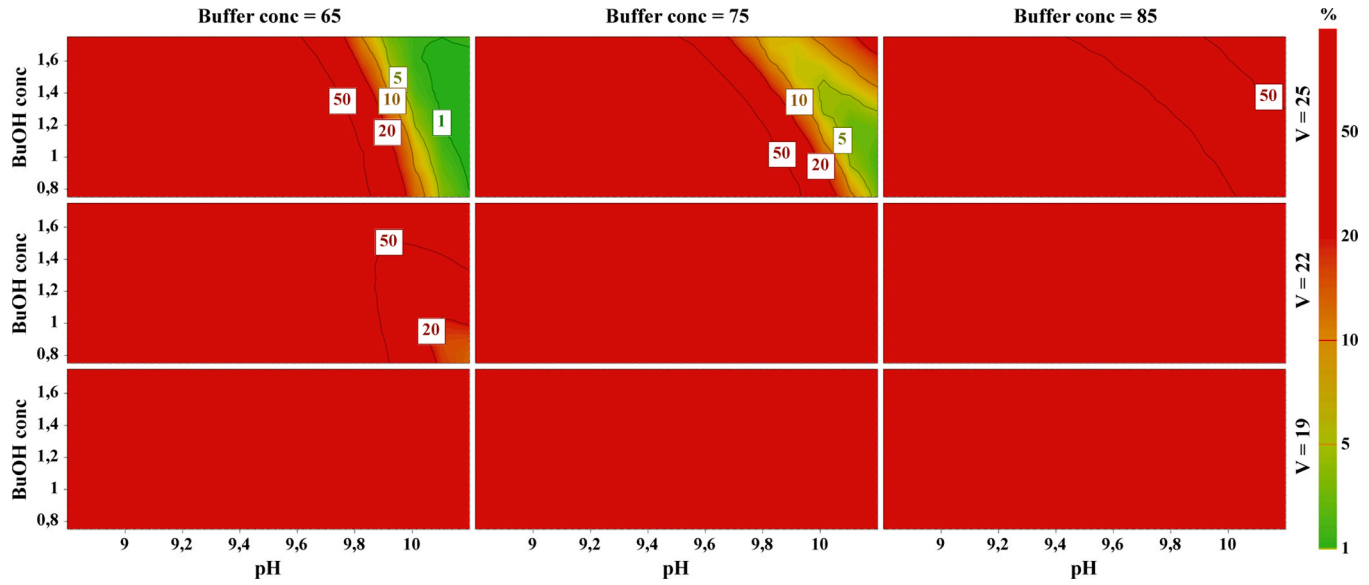


**Fig. 4.** Probability maps obtained plotting *BuOH conc vs. pH* at three different values of *Buffer conc* and *V*, with *SDS conc* at 105 mM. The 10 % isoprobability lines include the MODR, which is colored green.

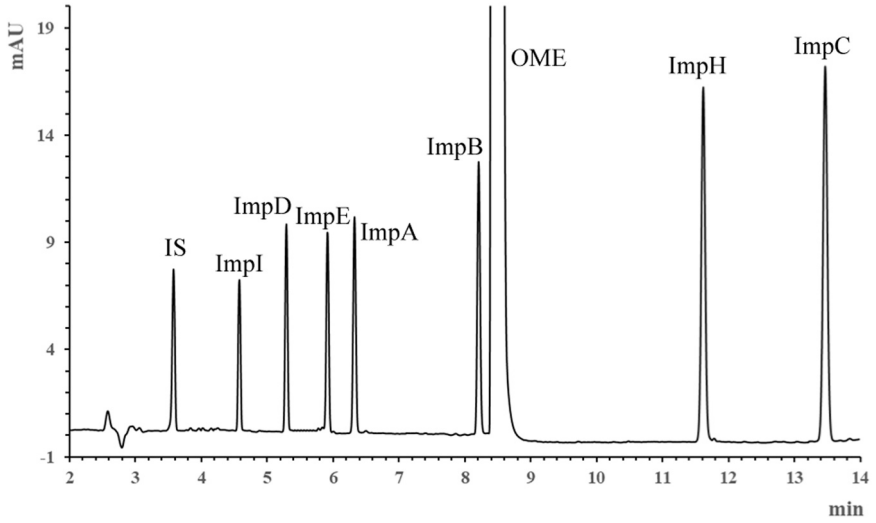


**Fig. 5.** Electropherogram in the optimized conditions. Test sample: OME 2 mg/mL, OME impurities 0.02 mg/mL, IS 0.04 mg/mL. Analytical conditions: 72 mM borate buffer pH 10.00, 96 mM SDS, 1.45 % v/v nBuOH; voltage, 25 kV; temperature, 21 °C. Capillary total length, 48.5 cm; capillary effective length, 40.0 cm. Detection wavelength, 200 nm.

variations were applied to the working point values of the CMPs to evaluate their impact on the CMAs. A linear model was hypothesized due to the small experimental domain, which was selected as follows: *Buffer conc*, 70–74 mM; *pH*, 9.90–10.10; *SDS conc*, 94–98 mM; *BuOH conc*, 1.35–1.55 %v/v; *V*, 24–26 kV; *T*, 20–22 °C. The Plackett-Burman experimental plan employed for estimating the CMPs effects is reported in Supplementary Table S4.

It is worth noting that all the parameters were studied in a narrower domain compared to the RSM, but always inside the tested RSM experimental range, with two exceptions. The first one was *V*, for which the optimum value was set at the higher limit of the experimental domain (25 kV); thus, it was necessary to extend the robustness study outside the RSM experimental range (26 kV). The second exception was *T*, which had been fixed according to the results obtained from the screening phase to 21 °C and thus did not undergo any further scrutiny in the RSM study.

Upon assessment, all the measured CMAs were inside the thresholds, aside from $R_6$ value in experiment no. 6, which was slightly lower than the target (≥1.3), but still allowing the determination of the two involved compounds ImpB and OME. At a first glance, a high variability in $R_8$ value could be also noticed; however, this did not represent a real analytical issue, because the separation was always guaranteed at resolution values much higher than the target (≥2.0).

Graphic analysis of the effects enabled to obtain detailed information on the statistical significance of the effects of the CMPs. The related plots are shown in Supplementary Fig. S7a-d, where the significant effects were pointed out using orange bars. Regarding $R_6$ and $R_8$, the significant effect of *pH* and *BuOH conc*, whose importance had been already pinpointed in RSM graphic analysis of effects (Supplementary Fig. S2), was confirmed even within this smaller domain. *pH* and *V* exerted an influential negative effect on $W_{OME}$. Instrumental parameters, such as *T* and *V*, as well as *Buffer conc*, were significant on *t*, albeit the latter to a lower extent with respect to the first two CMPs. Summarizing, robustness study highlighted that the correct setting of BGE parameters is

fundamental for the aspect of separation related to $R_6$. For all the other responses, including resolution $R_8$, the obtained values were well inside the thresholds and showed no criticalities. Thus, great attention should be focused on *pH* and *BuOH conc* values of the BGE, since these two CMPs have been shown to play a pivotal role in assuring a good separation.

The results from robustness study were used to outline the AP Method Control, which was accomplished through the definition of System Suitability Test [21]. When applying the working conditions to a standard text mixture of the compounds, the obtained values for the CMAs should be inside the intervals whose limits correspond to the lowest and the highest measured values in robustness test: $1.26<R6<2.12$; $11.24<R8<21.76$; $0.17<W_{OME}<0.29$; $11.07<t<14.52$.

### 3.8. Method validation and application

Validation was conducted in line with the ICH Q2(R2) guideline [27]. The evaluated Product Attributes included Assay Content for OME and Purity for the impurities. The Performance Characteristics assessed encompassed: Selectivity, Working Range (Suitability of Calibration model and, for the impurities, Quantitation Limits and Detection Limits), Accuracy, Precision. Further information can be found in Supplementary Information, including validation data in Supplementary Tables S5, S6 and S7. The developed AP was used to examine DP samples, which consisted in Omez® gastro-resistant capsules labelled to contain 20 mg OME. The analysis of the sample, obtained as described in Section 2.2, were done in triplicate ($n$=3, α=0.05), yielding 101.66 ±3.53 % recovery and 1.42 % RSD and the related electropherogram is shown in Supplementary Fig. S8a. The results aligned with the label's declared content and no impurities were detected above the limit of detection. The electropherogram from the pharmaceutical formulation spiked with the impurities at the Quantitation Limit level is reported in Supplementary Fig. S8b.

## 4. Conclusions

The development of a robust and efficient MEKC method for the simultaneous determination of OME and seven related impurities in DPs was successfully achieved through a systematic optimization approach. The AP was designed considering the need for baseline separation and sharp peak shapes. Several factors, including BGE composition, surfactant and organic modifier concentration, and CyDs addition were systematically evaluated using a combination of screening experiments and RSM.

Knowledge Management was used to select a suitable CE mode, opting for MEKC with borate and SDS as the buffer and surfactant, respectively. By integrating *n*-butanol as organic modifier, enhanced separation and better peak shapes were found. The MODR was defined and the optimal conditions for the MEKC method were identified: BGE, 72 mM borate buffer, pH 10.00, 96 mM SDS, 1.45 %v/v *n*-butanol, capillary temperature 21°C, applied voltage 25 kV. Under these conditions, the method provided good resolution between the impurities, sharp peak shapes and an analysis time of less than 14 min. The robustness of the AP was thoroughly assessed, ensuring its reliability and emphasizing the importance of carefully controlling pH and nBuOH concentration for maintaining a good resolution between the critical peak pair ImpB/OME.

The AP herein proposed is, to our knowledge, the only CE method in literature that encompasses all the Ph. Eur. listed impurities of OME, with the exception of the two ones (ImpF and ImpG) for which Ph. Eur. provides a spectrophotometric method. The importance of a systematic optimization process in AP development was highlighted, ensuring the method's effectiveness, robustness and applicability for routine analysis in QC laboratories. This study serves as another example of the value of AQbD, being in accordance with the most recent pharmaceutical analytical approaches described in ICH Q14 and Q2(R2). The successful development of a robust and efficient MEKC method for the simultaneous determination of OME and related impurities underscores the significance of systematic optimization and knowledge management in AP design.

## Funding

This study did not receive any specific grant from funding agencies in the public, commercial, or not-for-profit sectors.

## CRediT authorship contribution statement

**Adriana Modroiu:** Writing – original draft, Validation, Investigation, Formal analysis. **Gabriel Hancu:** Writing – review & editing, Supervision, Resources. **Roberto Gotti:** Writing – review & editing, Supervision, Conceptualization. **Serena Orlandini:** Writing – review & editing, Visualization, Supervision, Methodology, Data curation, Conceptualization. **Luca Marzullo:** Writing – original draft, Validation, Investigation, Data curation. **Sandra Furlanetto:** Supervision, Resources, Methodology, Conceptualization.

## Declaration of Competing Interest

The authors declare that they have no known competing financial interests or personal relationships that could have appeared to influence the work reported in this paper.

## Acknowledgements

The Authors wish to thank University of Medicine, Pharmacy, Science and Technology "George Emil Palade" of Târgu Mureș for supporting Adriana Modroiu's traineeship at the Department of Chemistry of the University of Florence in the context of the Erasmus+ Programme. The financial support provided by the MUR - Dipartimenti di Eccellenza 2023–2027 (DICUS 2.0) to the Department of Chemistry "Ugo Schiff" of the University of Florence is acknowledged.

## Appendix A. Supporting information

Supplementary data associated with this article can be found in the online version at doi:10.1016/j.jpba.2024.116295.

## References

[1] D.S. Strand, D. Kim, D.A. Peura, 25 years of proton pump inhibitors: a comprehensive review, Gut Liver 11 (2017) 27–37, https://doi.org/10.5009/gnl15502.
[2] R. Řemínek, F. Foret, Capillary electrophoretic methods for quality control analyses of pharmaceuticals: a review, Electrophoresis 42 (2021) 19–37, https://doi.org/10.1002/elps.202000185.
[3] European Pharmacopoeia, 11th Edition, Council of Europe, Strasbourg, 2023, pp. 3578-3579.
[4] C. Iuga, M. Bojita, S.E. Leucuta, Development of a validated RP-HPLC method for separation and determination of process-related impurities of omeprazole in bulk drugs, Farmacia 57 (2009) 534–541.
[5] K. Bastos Borges, A.J. Macías Sánchez, M. Tallarico Pupo, P. Sueli Bonato, I. González Collado, Ultra-fast gradient LC method for omeprazole analysis using a monolithic column: assay development, validation, and application to the quality control of omeprazole enteric-coated pellets, J. AOAC Int. 93 (2010) 1811–1820.
[6] S. Flor, V. Tripodi, S. Scioscia, L. Revello, S. Lucangioli, Fast and sensitive new HPLC-UV method for determination of omeprazole and major related substances in pharmaceutical formulation, J. Liq. Chromatogr. Rel. Technol. 33 (2010) 1666–1678, https://doi.org/10.1080/10826076.2010.519232.
[7] V.C. Manranjan, D.S. Yadav, H.A. Jogia, P.L. Chauhan, Design of Experiment (DOE) utilization to develop a simple and robust reversed-phase HPLC technique for related substances' estimation of Omeprazole formulations, Sci. Pharm. 81 (2013) 1043–1056, https://doi.org/10.3797/scipharm.1306-06.
[8] R.K. Seshadri, T.V. Raghavaraju, I.E. Chakravarthy, A single gradient stability-indicating Reversed-Phase LC method for the estimation of impurities in Omeprazole and Domperidone capsules, Sci. Pharm. 81 (2013) 437–438, https://doi.org/10.3797/scipharm.1209-12.

[9] L.K. Garg, S.S. Sait, T. Krishnamurthy, C.H.R.P. Kumar, Quality by Design (QbD): A practical experimental design approach by blocking and varying certain factors of a stability-indicating HPLC method for simultaneous determination of Omeprazole and Ketoprofen, J. Liq. Chromatogr. Relat. Technol. 38 (2015) 677–686, https://doi.org/10.1080/10826076.2014.951766.
[10] S. Koppala, V. Ranga Reddy, J.S. Anireddy, Development and validation of a novel stability-indicating RP-HPLC method for the simultaneous determination of related substances of Ketoprofen and Omeprazole in combined capsule dosage form, J. Chrom. Sci. 54 (2016) 765–775, https://doi.org/10.1093/chromsci/bmw008.
[11] A.H. Schmidt, M. Stanic, Rapid UHPLC method development for Omeprazole analysis in a Quality-by-Design framework and transfer to HPLC using chromatographic modeling, LC GC N. Am. 32 (2) (2014) 1–10.
[12] K. Kučerová, V. Reiská, F. Švec, L. Kujovská Krčmová, L. Matysová, Fast determination of omeprazole in extemporaneous suspensions used in paediatrics and stability studies, Anal. Methods 11 (2019) 517–523.
[13] E. Johansson, A. Karlsson, J.W. Ludvigsson, Ultra high performance liquid chromatography method development for separation of omeprazole and related substances on core-shell columns using a Quality by Design approach, J. Sep. Sci. 43 (2020) 696–707, https://doi.org/10.1002/jssc.201900726.
[14] S.B. Jadhav, C.Kiran Kumar, R. Bandichhor, P.N. Bhosale, Development of RP UPLC-TOF/MS, stability indicating method for omeprazole and its related substances by applying two level factorial design; and identification and synthesis of non-pharmacopoeial impurities, J. Pharm. Biomed. Anal. 118 (2016) 370–379, https://doi.org/10.1016/j.jpba.2015.10.005.
[15] J.J. Berzas Nevado, G. Castañeda Peñalvo, R.M. Rodríguez Dorado, V. Rodríguez Robledo, Study of controlled degradation processes and electrophoretic behaviour of omeprazole and its main degradation products using diode-array and ESI-IT-MS detection, Anal. Methods 5 (2013) 3299–3306.
[16] D. Agbaba, D. Novovic, K. Karljiković-Rajić, V. Marinković, Densitometric determination of omeprazole, pantoprazole, and their impurities in pharmaceuticals, JPC-J. Planar Chromatogr. 17 (2004) 169–172, https://doi.org/10.1556/jpc.17.2004.3.2.
[17] S. El Deeb, H. Wätzig, D. Abd El-Hady, C. Sänger-van de Griend, G.K.E. Scriba, Recent advances in capillary electrophoretic migration techniques for pharmaceutical analysis (2013–2015), Electrophoresis 37 (2016) 1591–1608, https://doi.org/10.1002/elps.201600058.
[18] M. Shah, N. Patel, N. Tripathi, V.K. Vyas, Capillary electrophoresis methods for impurity profiling of drugs: a review of the past decade, J. Pharm. Anal. 12 (2022) 15–28, https://doi.org/10.1016/j.jpha.2021.06.009.
[19] ICH Harmonised Tripartite Guideline, Pharmaceutical Development Q8(R2), 2009. ⟨https://database.ich.org/sites/default/files/Q8_R2_Guideline.pdf⟩ (Accessed 5 April 2024).
[20] P. Borman, K. Truman, D. Thompson, P. Nethercote, M. Chatfield, The application of Quality by Design to analytical methods, Pharm. Technol. 31 (2007) 142–152.
[21] S. Orlandini, S. Pinzauti, S. Furlanetto, Application of quality by design to the development of analytical separation methods, Anal. Bioanal. Chem. 405 (2013) 443–450, https://doi.org/10.1007/s00216-012-6302-2.
[22] E. Rozet, P. Lebrun, P. Hubert, B. Debrus, B. Boulanger, Design Spaces for analytical methods, Trends Anal. Chem. 42 (2013) 157–167, https://doi.org/10.1016/j.trac.2012.09.007.
[23] R. Deidda, S. Orlandini, P. Hubert, C. Hubert, Risk-based approach for method development in pharmaceutical quality control context: A critical review, J. Pharm. Biomed. Anal. 161 (2018) 110–121, https://doi.org/10.1016/j.jpba.2018.07.050.
[24] P. Borman, C. Campa, G. Delpierre, E. Hook, P. Jackson, W. Kelley, M. Protz, O. Vandeputte, Selection of analytical technology and development of analytical procedures using the analytical target profile, Anal. Chem. 94 (2022) 559–570, https://doi.org/10.1021/acs.analchem.1c03854.
[25] S. Orlandini, G. Hancu, Z.-I. Szabó, A. Modroiu, L.-A. Papp, R. Gotti, S. Furlanetto, New trends in the quality control of enantiomeric drugs, Quality by Design-compliant development of chiral capillary electrophoresis methods, Molecules 27 (2022) 7058, https://doi.org/10.3390/molecules27207058.
[26] ICH Harmonised Tripartite Guideline, Analytical Procedure Development Q14, 2023. ⟨https://database.ich.org/sites/default/files/ICH_Q14_Guideline_2023_1116.pdf⟩ (Accessed 5 April 2024).
[27] ICH Harmonised Tripartite Guideline, Validation of Analytical Procedures Q2(R2), 2023. ⟨https://database.ich.org/sites/default/files/ICH_Q2-R2_Document_Step2_Guideline_2022_0324.pdf⟩ (Accessed 5 April 2024).
[28] A. Dispas, H.T. Avohou, P. Lebrun, P. Hubert, C. Hubert, 'Quality by Design' approach for the analysis of impurities in pharmaceutical drug products and drug substances, Trends Anal. Chem. 101 (2018) 24–33, https://doi.org/10.1016/j.trac.2017.10.028.
[29] L. Marzullo, R. Gotti, S. Orlandini, P. Slavíčková, J. Jireš, M. Zapadlo, M. Douša, P. Nekvapilová, P. Řezanka, S. Furlanetto, Analytical Quality by Design-compliant development of a cyclodextrin-modified micellar electrokinetic chromatography method for the determination of trimecaine and its impurities, Molecules 28 (2023) 4747, https://doi.org/10.3390/molecules28124747.
[30] A. Modroiu, S. Krait, G. Hancu, G.K.E. Scriba, Quality by design-guided development of a capillary electrophoresis method for the chiral purity determination of silodosin, J. Pharm. Biomed. Anal. 222 (2023) 115117, https://doi.org/10.1016/j.jpba.2022.115117.
[31] S. Orlandini, R. Gotti, S. Furlanetto, Multivariate optimization of capillary electrophoresis methods: a critical review, J. Pharm. Biomed. Anal. 87 (2014) 290–307, https://doi.org/10.1016/j.jpba.2013.04.014.
[32] L. Eriksson, E. Johansson, N. Kettaneh-Wold, C. Wikström, S. Wold, Design of Experiments – Principles and Applications, MKS Umetrics AB, Umeå, Sweden, 2008.
[33] R. Yang, S.G. Schulman, P.J. Zavala, Acid-base chemistry of omeprazole in aqueous solutions, Anal. Chim. Acta 481 (2003) 155–164, https://doi.org/10.1016/S0003-2670(03)00076-X.
[34] C. Caprini, B. Pasquini, F. Melani, M. Del Bubba, A. Giuffrida, E. Calleri, S. Orlandini, S. Furlanetto, Exploring the intermolecular interactions acting in solvent-modified MEKC by Molecular Dynamics and NMR: The effect of *n*-butanol on the separation of diclofenac and its impurities, J. Pharm. Biomed. Anal. 149 (2018) 249–257, https://doi.org/10.1016/j.jpba.2017.11.010.
[35] M.A. Herrador, A.G. Asuero, A.G. Gonzalez, Estimation of the uncertainty of indirect measurements from the propagation of distributions by using the Monte-Carlo method: an overview, Chemom. Intell. Lab. Syst. 79 (2005) 115–122, https://doi.org/10.1016/j.chemolab.2005.04.010.